An experimental investigation of two different methods for swirl induction in a multivalve engine

E Pipitone and **U Mancuso**
Department of Mechanics (DIMA), University of Palermo, Palermo, Italy

The manuscript was received on 3 September 2004 and was accepted after revision for publication on 23 September 2004.

DOI: 10.1243/146808705X7365

Abstract: This paper describes an experimental investigation aimed at comparing the swirl effect induced by unbalancing the mass flow through the two intake ports of a multivalve engine head using two different methods: the first one reduced the curtain area of one of the intake valves [different lifts (DL) method]; the second one adopted a sluice-gate-shaped valve, installed upstream of the intake valves [swirl control valve (SCV) method] in order to cause a pressure drop. A steady-flow test rig (equipped with instrumentation for the discharge coefficient and swirl intensity measurement) was realized in order to compare and evaluate the results of both methods and determine their respective validity and limitations; the procedures used for both experimental methods are duscussed in detail. The flow characteristics were analysed through changes of lift difference or SCV position; it was found that both DL and SCV methods are effective in swirl induction but the DL mechanism, acting on the valve curtain area, is more effective in flow unbalancing between intake ports, since the flowrate depends linearly on the curtain area. The SCV method, instead, controls the port flowrate, inducing a localized pressure drop, whose intensity depends on the flow velocity in a non-linear manner. For this reason the SCV method can achieve strong swirl intensity only with high obstruction levels, in a narrow regulation window close to full-obstruction conditions.

Keywords swirl induction, multivalve engine, DL method, SCV method

1 INTRODUCTIN

It is well known that turbulent flow patterns are a critical factor in the combustion process and in determining the extent of mixing between fuel and air [**1**–**3**]. During the induction stroke the incoming flow is shaped by the geometrical characteristics of the induction port/intake valve assembly. The large-scale turbulent motions within the cylinder generated by the inlet port arrangement start to decay after closure of the intake valves, at a rate that strongly depends on their structure. A turbulent flow organized as rotation about the cylinder axis, known as 'swirl', is the most favourable in this respect, since its decay rate is lower than those of other turbulent flows; as a result to this, many induction systems are designed to produce swirl [**4**]. Moreover, experimental investigations [**5**–**7**] have shown a strong influence of swirl intensity on overall engine performance. Several design approaches are used to create swirl during the induction process [**1**]. Sometimes flow is discharged into the cylinder tangentially: a *directed port* brings the flow towards the valve opening in the tangential direction [Fig. 1(a)]. In other designs the swirl is generated within the inlet port, forcing the flow to rotate about the valve axis before it enters the cylinder: a *helical port* [Fig. 1(b)] can be used to obtain this flow structure. In other designs a non-uniform distribution of flow around the circumference of the inlet valve is forced in order to obtain a net angular momentum about the cylinder axis: *deflector ports* [Fig. 1(c)] and *shrouded wall ports* are used to force the flow preferentially in a tangential direction.

Another technique for swirl induction is based flow unbalancing between intake ports. Several swirl induction systems based on total or partial obstruction of one of the inlet ports, obtained through a butterfly-type swirl control valve [**7**–**10**], are reported. Using one of these methods, several experimental investigations were performed in order to find out geometrical parameters for swirl induction [**6**, **11**, **12**].

* *Corresponding author: Department of Mechanics (DIMA), University of Palermo, Viale delle Scienze, Palermo, 90128, Italy. email: pipitone@dima.unipa.it*

EN00004203 09-12-04 09:03:28 Rev 14.05
The Charlesworth Group, Huddersfield 01484 517077

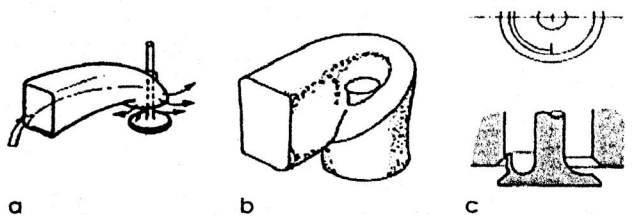

Fig. 1 Swirl port designs

In the present work the authors investigate the effect of two different methods for swirl flow induction based on flow unbalancing between the two inlet ports of a four-valve single-cylinder engine head; both methods are applicable even if the intake port geometry is already established by the design process and swirl is induced, forcing the flow distribution to be non-uniform between the intake ducts, thus causing the inlet flow to have a net angular moment about the cylinder axis. In this paper the flow structure is achieved in two ways: using the different lifts (DL) method for intake valves or using a partial obstruction of one of the inlet ports by means of a sluice gate installed upstream of the inlet valve [the swirl control valve (SCV) method]. The former method induces flow unbalancing by means of valve curtain area reduction, while the latter acts by inducing a localized pressure drop upstream of one of the intake valves. The effect of these different methods on swirl flow generation, together with their influence on the engine breathing capacity, was investigated and will be discussed below. The purpose of the present work is to provide useful information for selection of the most suitable swirl generation method to use for different design problems. The information provided is expected to be useful to engineeers working on the development of cylinder heads, since the trade-off between turbulence generation and breathing performance of the two examined methods (which are simple, low cost, and easy to package on new and existing engines) is clearly stated by means of a direct comparison. The improvement in fuel consumption under partial load conditions, without compromising performance or noxious emissions, is a major issue in the development of lean-burn engines. This task can be pursued by adopting the optimized swirl ratio for every load and speed conditions by means of a variable-swirl system, based, for example on the DL or SCV methods.

2 EXPERIMENTAL SYSTEM

As the nature of swirling flow in an actual operating engine is very difficult to observe, steady-flow benches are often used to characterize the swirl flow and the breathing performances of the engines. The main disadvantage of steady tests relates to a lack of information about the in-cylinder flow structure, which is always unsteady, but is balanced by many advantages, such as the simple flow block hardware, rapid testing, and easily interpreted output in the form of the flow coefficient and swirl ratio. Even if the relationship between steady-flow rig tests and actual engine swirl patterns is not straightforward, due to the unsteady behaviour of the transient flow field and to the superimposed piston motion, steady-flow tests adequately describe the swirl-generating characteristics of the intake system at a fixed valve lift, and are extensively used for this purpose [**1**]. Moreover, the flow bench test of a cylinder head is particularly useful for choosing the best trade-off between the engine flow capacity and the swirl strength. Despite the diversity in experimental configurations, there is evidence that steady-flow tests correlate well with real engine combustion performances [**13**]. For this reason the experimental tests were carried out on a steady-flow rig.

2.1 Experimental set-up

The steady-flow rig realized for this study, including the cylinder head, test sections, and suction system is show schematically in Fig. 2. To perform the experiments, a pent-roof four-valve single-cylinder engine head ① was employed; the head overall dimensions are summarized in Table 1. Each intake valve was equipped with a dial gauge ② for fine lift tuning. A swirl control valve was installed upstream of one of the inlet ports. A straight pipe was connected downstream of the cylinder head, and was employed as the main test section. A few bore diameters down the cylinder head (see section 2.3) a paddle-wheel swirlmeter ③ was fitted into the pipe. A centrifugal compressor ⑥ was used to provide airflow, which was controlled using a butterfly-type valve ⑦ and a by-pass valve ⑧. Two main measurement sections were installed: in the first (section 1 in Fig. 2) the pressure and temperature were measured, 10 diameters downstream of the swirlmeter, in order to minimize flow disturbances due to the

Table 1 Overall dimensions of the head

Parameter	Value
Bore (mm)	94
Number of intake valves	2
Number of exhaust valves	2
Intake valve seat diameter (mm)	36
Intake valve angle (deg)	65

EN00004203 09-12-04 09:03:28 Rev 14.05
The Charlesworth Group, Huddersfield 01484 517077

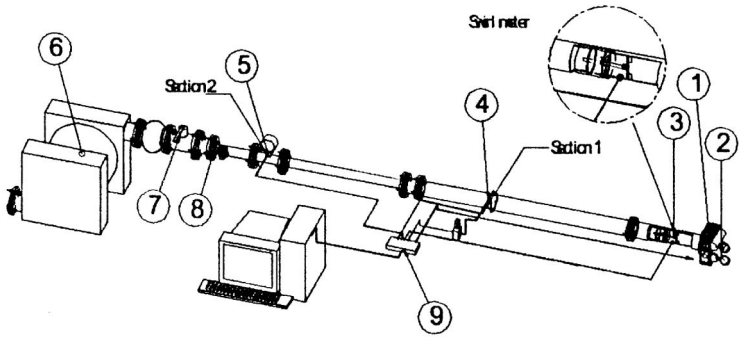

Fig. 2 Steady-flow rig

passage through the engine head and the swirlmeter; the other main section provided the mass flow measurement (section 2) by the use of a vortex flowmeter ⑥. Signal acquisition was performed using a National Instruments DAQ board ⑨ interfaced with LabVIEW software.

2.2 Swirlmeter

A paddle-wheel anemometer was used to measure swirl under steady-flow conditions. This kind of measurement system presumes the flow to have a solid body structure, which means that tangential velocity depends linearly on the distance from the rotation axis. Due to the head friction and shape, in-cylinder flow can be different from the solid-body rotational structure; however, several experimental investigations [**12**] have shown that the swirl structure tends to a solid-body structure as it goes away from the head. An uncertainty is introduced by the rotating friction torque, but it was found to be negligible. [The greatest friction torque for the maximum axial load and revolving speed observed is approximately 0.1 N mm (SKF technical specification for 618/6 rolling bearings), which is about 0.3 per cent of the flow angular momentum at the same operating conditions.] Moreover, the aim of the present work is to compare two methods for swirl induction, rather than give a precise measure of the respective swirl intensities. The paddle wheel used is composed of two steel blades supported by a low friction bearing, which is fitted in a steel axle and kept in its concentric locating by means of a frame fitted into the straight pipe downstream of the cylinder head. Each component was accurately designed in order to reduce the pressure drop as much as possible, and this allowed the simultaneous measurement of discharge and swirl coefficients (as can be seen in Fig. 2, the pressure measurement section is downstream of the swirlmeter). A typical test procedure involved the measurement of the paddle rotational speed for a series of intake port geometries and pressure drops across the cylinder head. The rotational speed readings, measured using a magnetic pick-up mounted outside the pipe, were used to compute the angular velocity of the equivalent rotating solid body. The wide range of experimental data found provides an estimation of the in-cylinder axial swirl ratio at the end of the induction process. With regards to the position of the swirl measurement plane, several authors have shown that the flow field varies along the cylinder axis. Fitzgeorge and Allison [**14**] found that by placing the paddle-wheel anemometer between 0.8 and 1.4 times of the cylinder bore away from the cylinder head, a fully developed swirl can be measured. Heywood [**1**] suggests the use of a paddle wheel mounted between 1 and 1.5 times the cylinder bore down the cylinder. Oishi *et al.* [**15**] and other authors [**10**, **16**], show that a stable swirl motion can be observed at approximately 1.75 times the cylinder bore downstream of the cylinder head. Some preliminary tests were performed and confirmed this position to be the optimum for the swirl measurement plane (Fig. 3).

The main goal of this work was to evaluate DL and

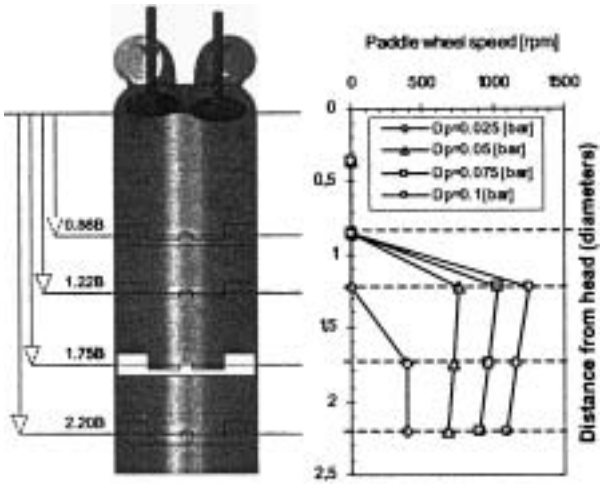

Fig. 3 Swirl measurement plane positioning ($h_1 =$ 4 mm, $h_2 = 6$ mm) for various pressure drops Δp

EN00004203 09-12-04 09:03:28 Rev 14.05
The Charlesworth Group, Huddersfield 01484 517077

SCV systems in terms of swirl intensity and the discharge coefficient, and to compare the results of both methods in order to determine their respective validity and limitations. To achieve such objectives several parameters, shown below, were used.

2.3 Swirl measurement

The main issue in swirl analysis is related to selection of the proper swirl parameter. The only widely adopted hypothesis is that the flow can be treated as a solid-body vortex with a uniform axial velocity. Heywood [**1**] suggested a swirl coefficient that takes into account the equvalent solid-body angular velocity

$$C_{\text{swirl}} = \frac{\omega B}{v_0} \tag{1}$$

where B is the cylinder bore, ω is the paddle-wheel rotational speed, and v_0 is the ideal curtain area flow velocity, derived from the isentropic pressure drop across the valve. At a fixed pressure drop across the engine head, v_0 is a constant, so this swirl coefficient depends only on the paddle-wheel rotational speed and does not take the discharge coefficient into account.

Another widely adopted swirl intensity parameter is the swirl ratio S_{r}, defined as the angular velocity of the solid body rotating flow ω, which has the same angular momentum as the actual flow, divided by the engine crankshaft angular rotational speed ω_{engine}

$$S_{\text{r}} = \frac{\omega}{\omega_{\text{engine}}} \tag{2}$$

For steady state flow a fictitious crankshaft angular rotational speed is defined as the rotational speed of the engine that induces the mean mass flow G during one induction stroke. Adopting such a definition, the swirl ratio appears to be proportional to the ratio between the tangential and axial velocity components at the external radius of the cylinder, and can be calculated from

$$S_{\text{r}} = \frac{\rho_1 V \omega}{30\,G} \propto \frac{w}{u} \tag{3}$$

where ρ_1 is the air density in the pressure measurement section, V is the engine displacement, w is the tangential velocity component, and u is the axial velocity component. Since the goal of the present work is to determine the intensity of swirl related to changes in geometry of the admission branch rather then to determine the optimum trade-off between swirl induction and breathing capability, both definitions for the swirl parameter were used, while the resistance to the flow of the inlet/port valve system was separately taken into account through the calculation of the discharge coefficient (see section 2.4).

2.4 Flow measurement

The breathing capability of the head can be quantified by calculating the discharge coefficient and the relative flow ratio. The discharge coefficient is defined as the ratio of the actual mass flow to the ideal mass flow passing through an isentropic nozzle in the same boundary conditions; it accounts for fluid dynamic losses across the engine head. The choice of the area to consider for ideal mass flow calculation is arbitrary, and various reasonable choices exist. The most widely used is the curtain area, the lateral surface of the cylinder having a diameter and height respectively equal to the valve seat diameter and lift. Since the pressure drop finished just downstream of the curtain area, the discharge coefficient can be calculated as

$$C_{\text{e}} = \frac{G}{A_{\text{c}}\sqrt{2\dfrac{k}{k-1}p_0\rho_0\left[\left(\dfrac{p_1}{p_0}\right)^{2/k} - \left(\dfrac{p_1}{p_0}\right)^{(k+1)/k}\right]}} \tag{4}$$

where A_{c} is the total curtain area, k is the isentropic coefficient, ρ_0 and p_0 are the ambient density and pressure and p_1 is the downstream static pressure measured in section 1 (see Fig. 2). The pressure downstream of the valve seat was assumed to be the same in the measurement section 1 since the pressure drop induced by the paddle wheel was negligible (at most 2 per cent of the total pressure drop, which in turn means a 1 per cent error in the discharge coefficient evaluation).

Some experimental evaluations confirmed that the mass flowrate mainly depends on the total curtain area A_{c}. Figure 4 shows the linear correlation between the mass flowrate and the sum of the valve lifts (which is proportional to the total curtain area) at a nominal pressure drop of 10 000 Pa.

The relative flow ratio $C_{\text{e,rel}}$, defined as the ratio of the actual mass flow to the mass flow discharged by the head in the original configuration (SCV wide open, equal valve lifts), can be used to evaluate the discharge coefficient reduction caused by the swirl induction mechanism. Figure 5 shows swirl intensity and the relative flow ratio for a DL arrangement ($h_1 = 3$ mm, $h_2 = 1.2$ mm). It can clearly be seen that a loss in breathing capacity of 35 per cent is necessary to achieve a swirl ratio of approximately 0.65.

EN00004203 09-12-04 09:03:28 Rev 14.05
The Charlesworth Group, Huddersfield 01484 517077

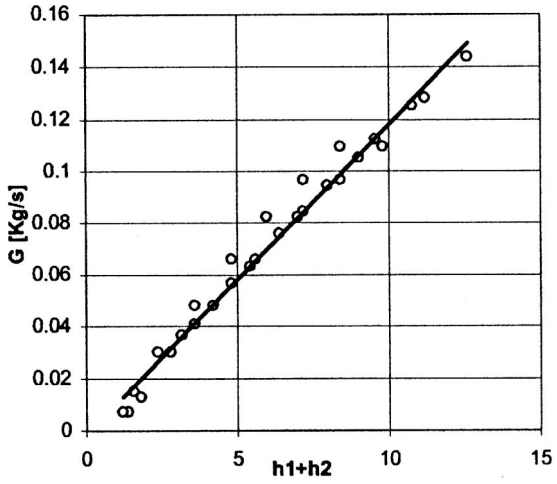

Fig. 4 Linear correlations between the mass flowrate and the sum of the valve lifts for $\Delta p = 10\,000$ Pa

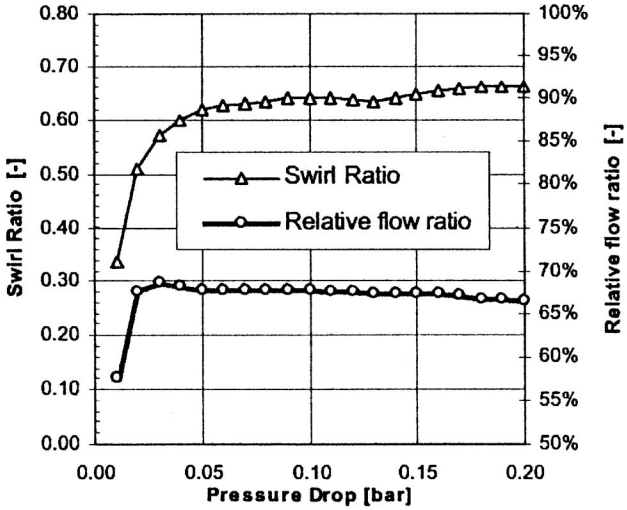

Fig. 5 Swirl ratio and relative flow ratio for a DL arrangement

3 EXPERIMENTAL RESULTS

The experimental tests were carried out while fixing the geometrical parameters of the intake ports (valve lifts and positions of swirl generation devices) at various pressure drops. Three distinct cycles of experimental tests were carried out, allowing a wide range of data to be collected. The first investigation was carried out to obtain the fluid dynamic characterization of the head in the original configuration, i.e. with equal valve lifts and wide-open swirl control valves. The second experimental test was carried out to evaluate swirl turbulence induction and breathing capability of the head under the DL configuration (Fig. 6), while in the third cycle of investigations the same information was obtained with the SCV configuration (Fig. 7). Both DL and SCV methods induce

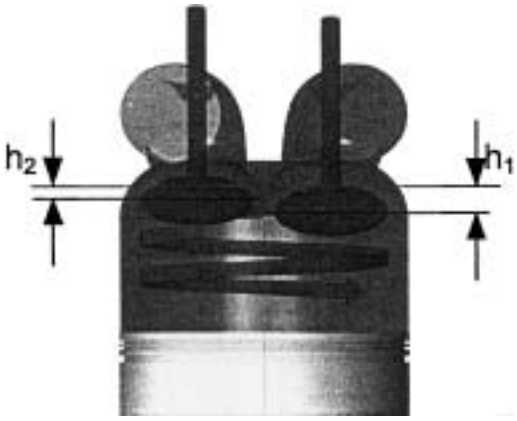

Fig. 6 Different lifts arrangement

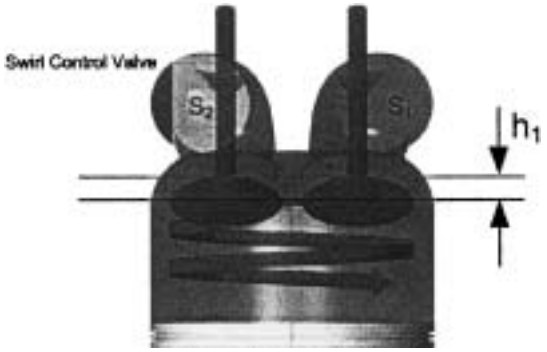

Fig. 7 Swirl control valve management

swirl turbulence, forcing the flow distribution to be non-uniform between the two intake ports; for this reason a geometrical parameter, the *throttling factor*, was defined in order to characterize the flow unbalancing between inlet ducts.

For the SCV arrangement the throttling factor is defined as the ratio between the closed area and the inlet area of the clear intake port (S_1 in Fig. 7)

$$\frac{\Delta S}{S_1} = \frac{S_1 - S_2}{S_1} \tag{5}$$

For the DL arrangement the throttling factor is defined by referring to the curtain areas of the two intake ports. Since these are proportional to valve lifts, it can be expressed as the difference between the lifts of the intake valves divided by the base lift h_1 in order to obtain a dimensionless parameter

$$\frac{\Delta S}{S_1} = \frac{h_1 - h_2}{h_1} = \frac{\Delta h}{h_1} \tag{6}$$

The experimental investigations were performed using the throttling factor as a base geometrical parameter for the composition of the two methods, adopting base lift values up to 7 mm and throttling

EN00004203 09-12-04 09:03:28 Rev 14.05
The Charlesworth Group, Huddersfield 01484 517077

factor values between 0.2 and 0.8. The results of a single test procedure are shown in Fig. 5.

Many early works show that the main requirement for the flow bench steady test is that the flow should be fully turbulent so that the friction factor across the intake ports is independent of the Reynolds number. As a consequence, the discharge coefficient becomes insensitive to pressure drop and mass flowrate; this can be seen in Fig. 8 for a pressure drop exceeding 2500 Pa.

Ricardo [**18**] showed that a fully turbulent flow can be obtained when the 'port Reynolds number' exceeds 60.000 at low valve lifts or 90.000 at high valve lifts. To ensure this condition, pressure drops in the range of 2500–10 000 Pa were chosen for a performance comparison between DL and SCV methods.

3.1 Different lifts method

The experimental investigations confirmed that swirl intensity increased according to the throttling factor, as shown in Fig. 9, for several values of h_1 at the nominal pressure drop of 5000 Pa. It can be observed that the highest values of swirl ratio are obtained at a throttling factor close to 1. This geometrical configuration leads to the full closure of one of the intake ports. In such a situation a heavy loss in breathing capability is the price for strong swirl induction. For lower values of $\Delta h/h_1$ it is possible to obtain intermediate values of swirl ratio, with better breathing performances. It was also observed that, while the mass flowrate depends linearly (see Fig 4) on the curtain area, the swirl ratio grows exponentially with curtain area reduction. Figures 10 to 12 show the loss in breathing capability in comparison with swirl turbulence induced for several values of the throttling factor $\Delta h/h_1$, grouped by pressure drop. Except for very low valve lifts, once the throttling factor and pressure drop are fixed, changes of valve lift do not affect the relative flow ratio significantly. This can be explained by remembering that the mass flow depends mainly on the total curtain area (Fig. 4).

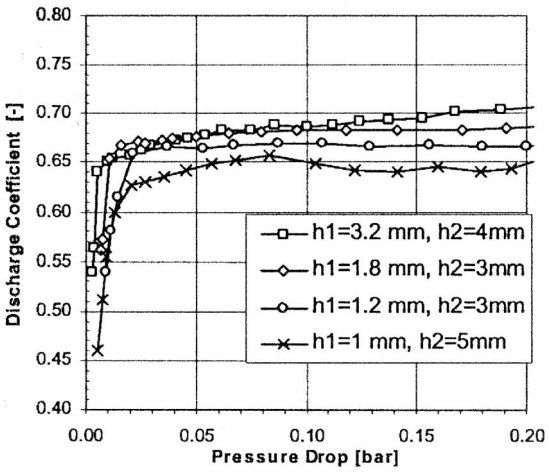

Fig. 8 Discharge coefficient saturation for several configurations of the intake ports

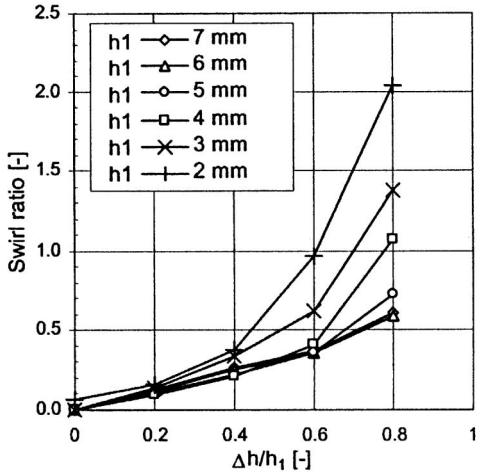

Fig. 9 Correlation between the swirl ratio and the throttling factor at the nominal pressure drop of 5000 Pa

3.2 Swirl control valve arrangement

In order to compare the DL method with a more common swirl induction technique based on the same mechanism (flow unbalancing between the two intake ports), an experimental investigation on the SCV method was carried out. Several tests performed with the SCV arrangement confirmed that swirl intensity increased according to the throttling factor. Figure 13 shows the correlation between the swirl ratio and the throttling factor, for several values of h_1 (pressure drop of 5000 Pa).

The comparison between Figs 9 and 12 shows a wider variation of swirl ratio with valve lift for the DL method with respect to the SCV arrangement. The DL method, in fact, induces a strong flow unbalance, reducing the valve curtain area. This shows a dependence of the swirl ratio on mass flow G and, hence, indirectly on the base lift h_1. The swirl ratio, which is proportional to the ratio between tangential and axial velocity components of the flow, is amplified by the reduction in the axial velocity component at low valve lifts and high obstruction factors $\Delta h/h_1$. The SCV method behaves in a slightly different way. At a fixed base lift, the influence of $\Delta S/S_1$ on mass flow is less sharp and the previously mentioned amplification effect is not present. This can be confirmed by observing the relative flow ratios for both methods. Figures 14 to 16 show the relative flow ratio and the swirl coefficient C_{swirl} for several base lifts h_1

EN00004203 09-12-04 09:03:28 Rev 14.05
The Charlesworth Group, Huddersfield 01484 517077

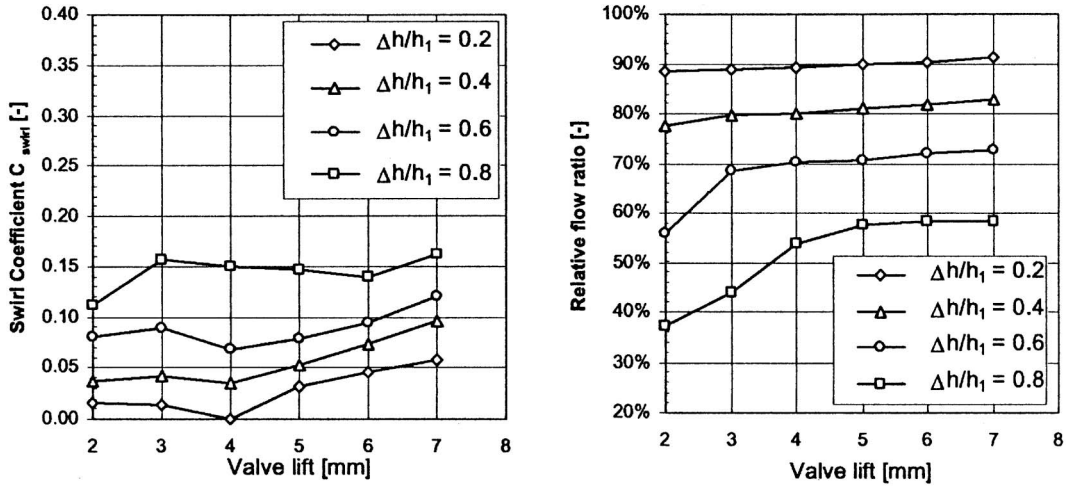

Fig. 10 DL: swirl coefficient and relative flow ratio at $\Delta p = 2500$ Pa

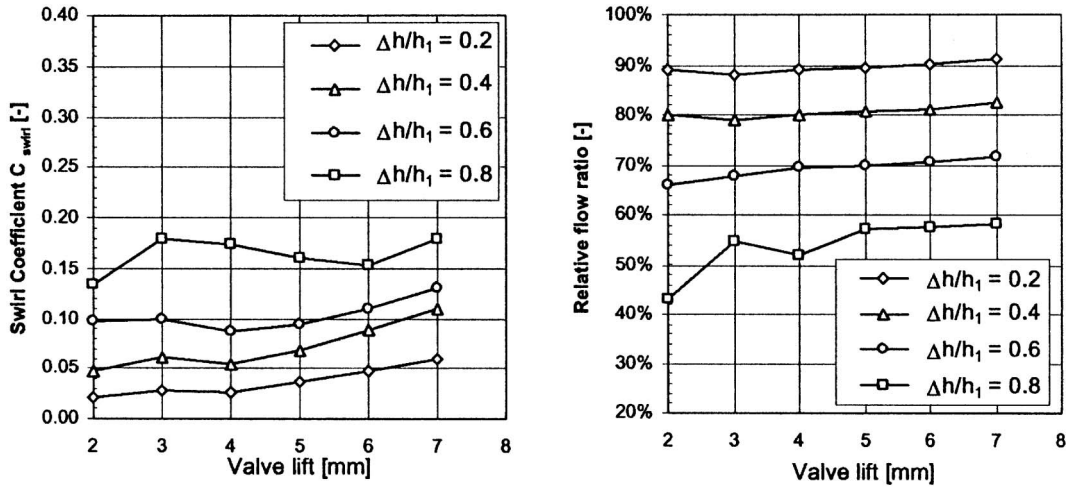

Fig. 11 DL: swirl ratio and relative flow ratio at $\Delta p = 5000$ Pa

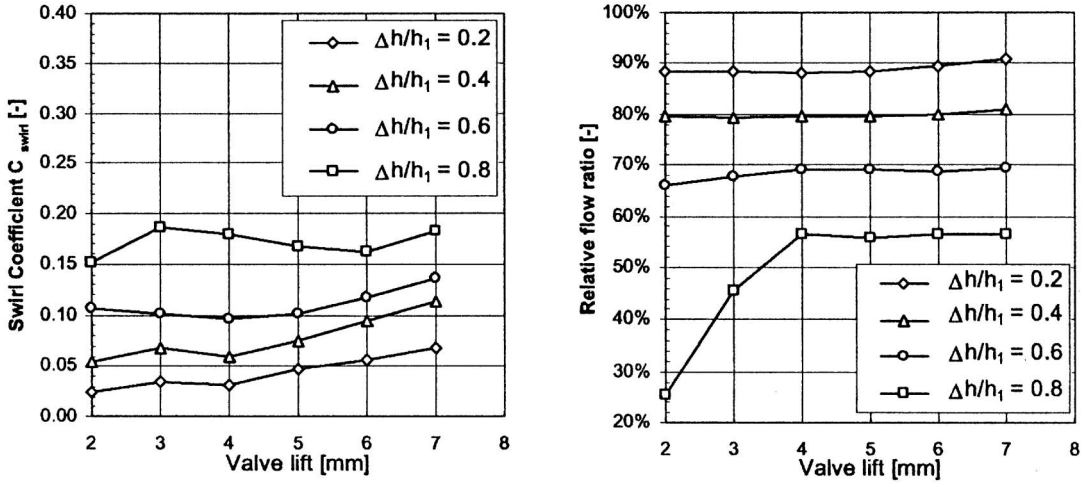

Fig. 12 DL: swirl ratio and relative flow ratio at $\Delta p = 10\,000$ Pa

EN00004203 09-12-04 09:03:28 Rev 14.05
The Charlesworth Group, Huddersfield 01484 517077

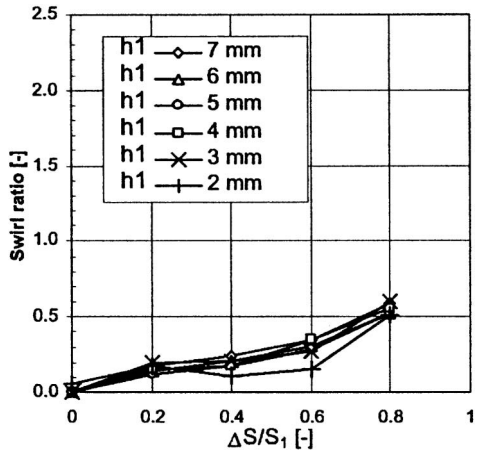

Fig. 13 Correlation between the swirl ratio and the obstruction factor (pressure drop of 5000 Pa)

and for the throttling factor up to 0.8, grouped by pressure drop. As in the previous case, the maximum swirl intensity is achieved at a nominal pressure drop of about 10 000 Pa.

Hamamoto *et al.* [**19**] found that the effect of swirl on combustion in a cylinder can be expresses as a function of the turbulence intensity, and that a strong dependence between combustion behaviour and swirl ratio S_r can be observed. Figure 17 shows the burn duration to decreae greatly while the swirl ratio increases. Figures 18 to 20 show a comparison between the DL and SCV methods by means of these parameters.

4 DISCUSSION

The experimental investigations confirmed the possibility of inducing swirl turbulence through a flow

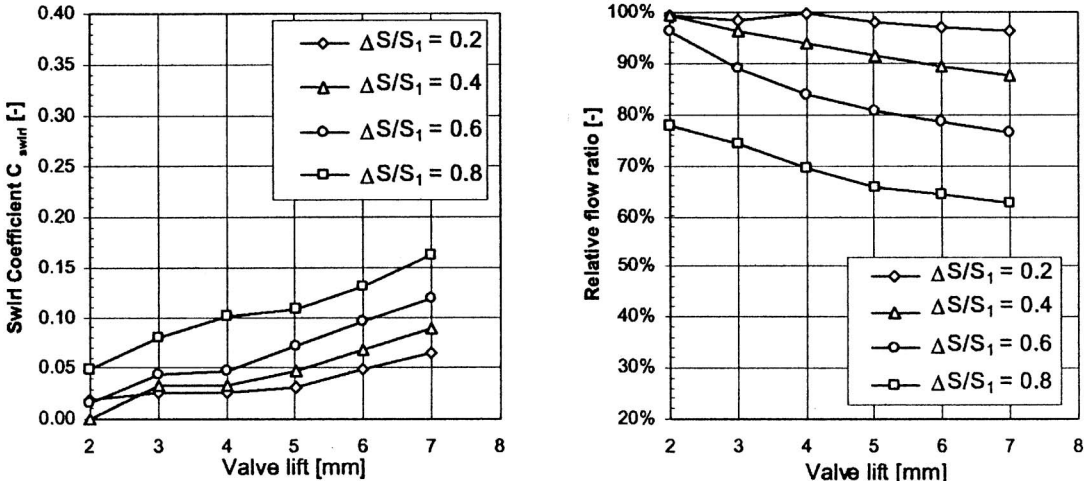

Fig. 14 SCV: swirl coefficient and relative flow ratio at $\Delta p = 2500$ Pa

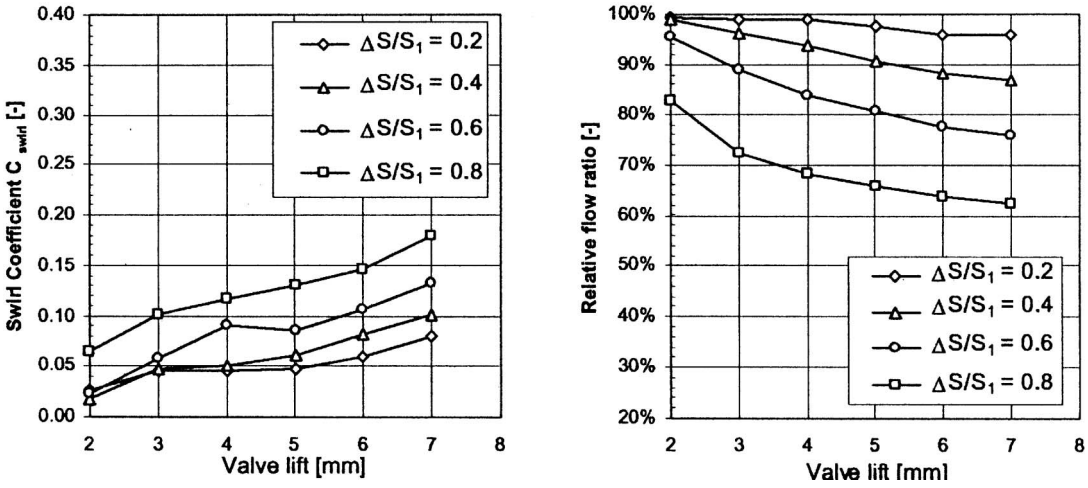

Fig. 15 SCV: swirl coefficient and relative flow ratio at $\Delta p = 5000$ Pa

EN00004203 09-12-04 09:03:28 Rev 14.05
The Charlesworth Group, Huddersfield 01484 517077

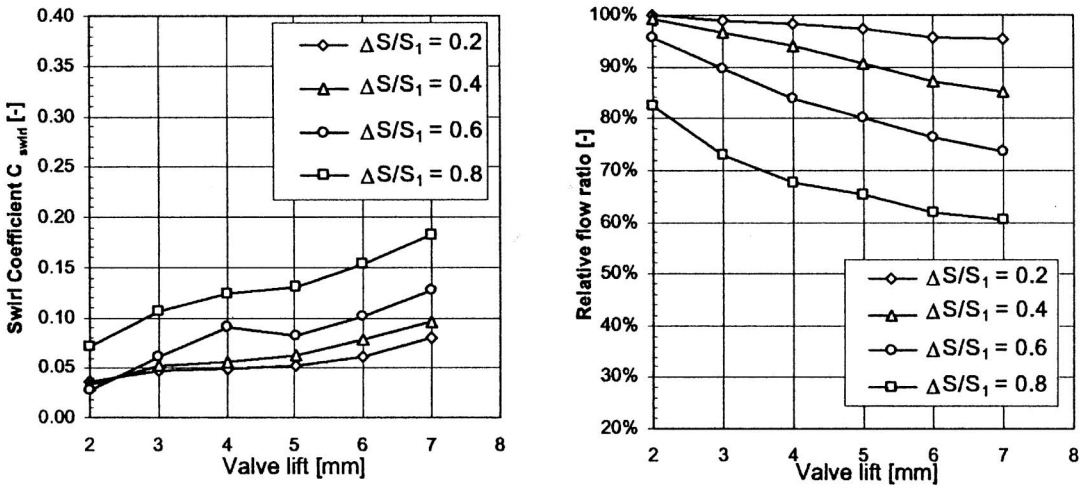

Fig. 16 DL: swirl coefficient and relative flow ratio at $\Delta p = 10\,000$ Pa

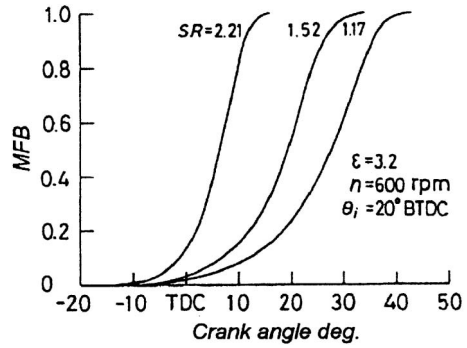

Fig. 17 Comparison of the mass fraction burned for three different swirl ratios (drawn from Hamamoto *et al.* [**19**])

unbalancing between the two intake ports, realized by means of two different methods: a direct method (DL method) that reduced the curtain area of one of the two inlet ducts and an indirect method (SCV method) that created flow unbalancing by means of a localized pressure drop upstream of one of the intake valves. The strong dependence of the relative flow ratio on the area of the intake section has been also shown; for both methods this area is the total curtain area A_c, which is

$$A_c^{DL} = \pi d_v h_1 \left(2 - \frac{\Delta S}{S_1}\right) \tag{7}$$

in the DL method and

$$A_c^{SCV} = 2\pi d_v h_1 \tag{8}$$

in the SCV arrangement. With a fixed throttling factor, the SCV curtain area is in any case wider than the DL curtain area, thus producing an unbalancing effect for the SCV method, which led to better breathing performances and consequently to lower swirl ratios. Fixing attention on a geometrical configuration characterized by a base lift $h_1 = 6$ mm, the differences between the DL and SCV methods in terms of swirl induction and breathig capability can be clearly shown (Fig. 21).

Even if both methods are effective in inducing swirl turbulence, it can be seen that (Fig. 22) higher swirl intensity can be achieved with the DL arrangement. Naturally a different impact on the breathing capability of the head was found for the two arrangements (Fig. 22).

Comparing the DL and SCV methods on this basis, their different behaviours can be observed. The DL mechanism, acting on the valve curtain area, is more efficient in flow unbalancing between the intake ports, and seems to control swirl intensity smoothly and in a wide operative range, also a low valve lift. This could lead to an effective swirl induction even in the first phase of the inlet stroke. The second method controls indirectly and, together with the valves, lifts the flow unbalance owing to the localized pressure drop dependence on the mass flow through the intake ports. Thus, owing to its dissipative behaviour, the SCV method has a narrow operative range, corresponding to high obstruction levels near the full closure of one intake duct.

5 CONCLUSION

A series of steady-flow tests were performed for two different swirl induction methods based on the flow unbalancing between the two intake ducts of a multivalve engine head, obtained by means of two different geometrical configurations [different lifts (DL) and swirl control valve (SCV) methods]. These

EN00004203 09-12-04 09:03:28 Rev 14.05
The Charlesworth Group, Huddersfield 01484 517077

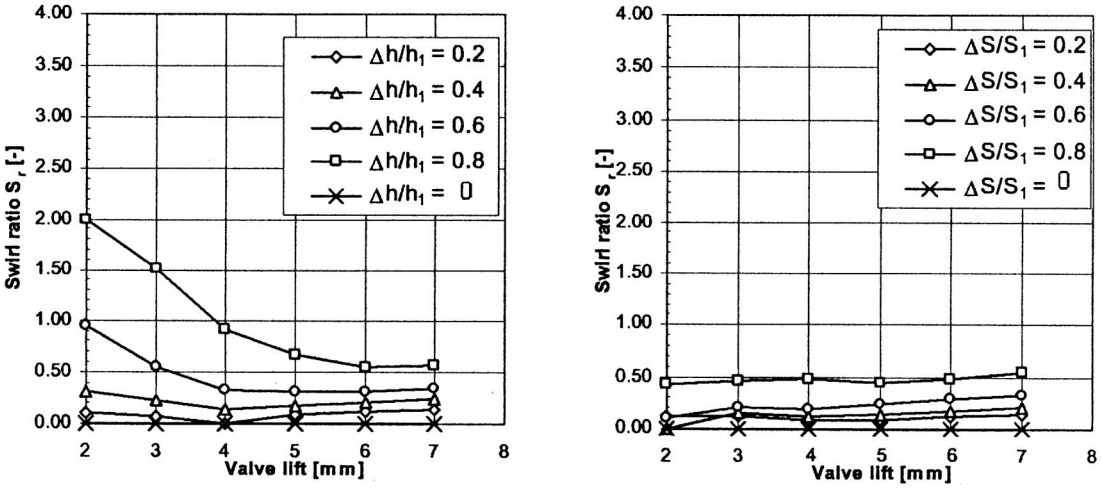

Fig. 18 Swirl ratio at $\Delta p = 2500$ Pa for DL (left) and SCV (right) methods

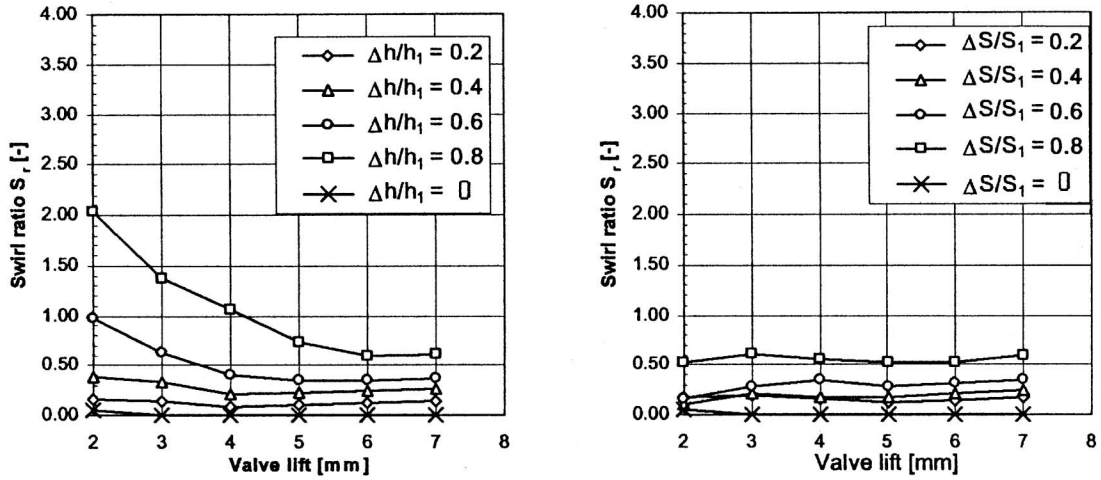

Fig. 19 Swirl ratio at $\Delta p = 5000$ Pa for DL (left) and SCV (right) methods

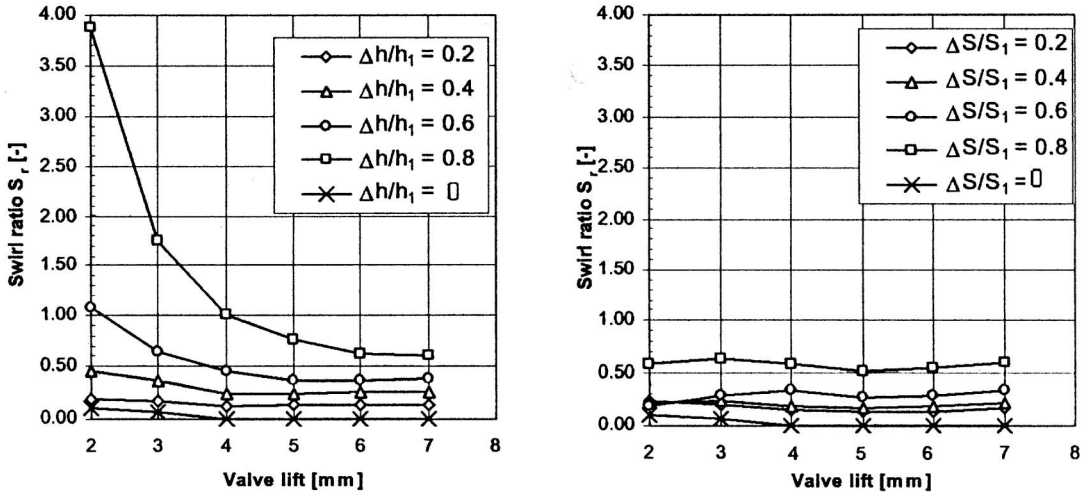

Fig. 20 Swirl ratio at $\Delta p = 10\,000$ Pa for DL (left) and SCV (right) methods

EN00004203 09-12-04 09:03:28 Rev 14.05
The Charlesworth Group, Huddersfield 01484 517077

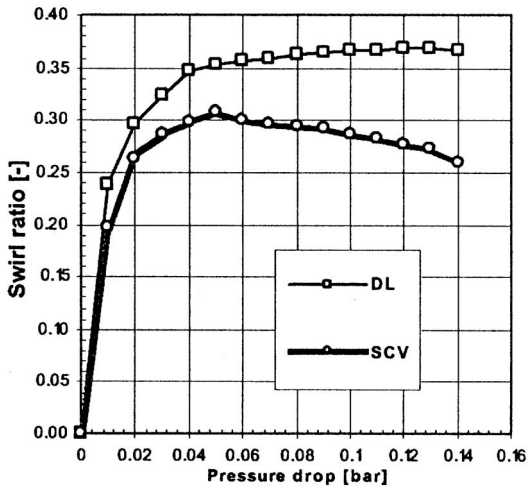

Fig. 21 Swirl ratio at $\Delta S/S_1 = 0.6$, $h_1 = 6$ mm for DL and SCV arrangements

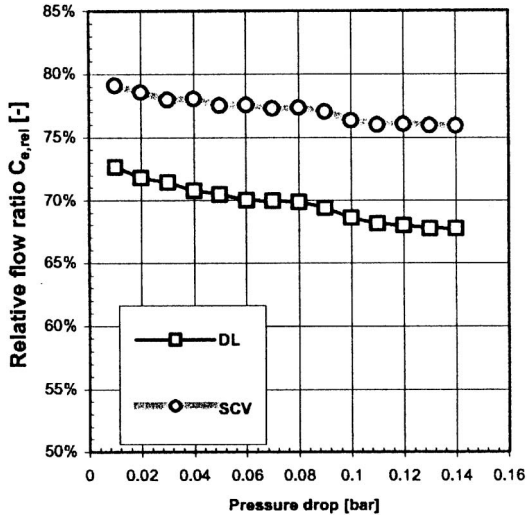

Fig. 22 Relative flow ratio at $\Delta S/S_1 = 0.6$, $h_1 = 6$ mm for DL and SCV arrangements

experimental investigations were performed for a wide range of flow conditions and valve lifts; both methods confirmed the possibility of obtaining a strong swirl turbulence. The flow characteristics have been analysed through changes in the SCV opening and different lifts arrangement, both measured by a throttling factor. The SCV-controlled swirl ratio varied from zero to 0.58, while the DL arrangement permitted a swirl ratio of 3.9 to be reached. The swirl ratio was found to be correlated to the throttling factor and a different impact on the breathing capability of the head was found for the DL and SCV methods, due to the larger flow passage area of the SCV arrangement. It was found that both DL and SCV methods are effective in swirl induction, but the DL mechanism, acting on the valve curtain area, is more effective in flow unbalancing between intake ports and controls swirl in a wide operative range. The SCV method, however, has a narrow operative range, corresponding to high obstruction levels near to the full closed duct condition. For this reason the DL system permits a smoother and wider swirl intensity control than the SCV system, which, though its simplicity makes it an attractive swirl induction method, seems to be less effective.

ACKNOWLEDGEMENTS

This research has been supported by the Italian Ministry for University Research (MURST). The authors would like also to express appreciation to Mr Benjamin Drago for his invaluable technical support.

REFERENCES

1 **Heywood, J.** *Internal Combustion Engine Fundamentals*, 1988 (McGraw-Hill, New York).
2 **Lee, K., Park, D.** and **Kim, C.** Effect of charge motion on flame kernel behavior and flame propagation. SAE technical paper 9530373, 1995.
3 **Zhang, D.** and **Hill, P. G.** Effect of swirl on combustion in a short cylindrical chamber. *Combust. Flame*, 1996, **106**(3), 318–332.
4 **Horlock, J. H.** and **Winterbone, D. E.** *The Thermodynamics and Gas Dynamics of Internal Combustion Engines*, Vol. II, 1986 (Oxford Science Publications, New York).
5 **Wang, H. W., Zhou, L. B., Jiang, D. M.** and **Huang, Z. H.** Study on the performance and emissions of a compression ignition engine fuelled with dimethyl ether. *Proc. Instn Mech. Engnrs, Part D: J. Automobile Engineering*, **214**(D1), 101–106.
6 **Kang, K.** and **Reitz, Z.** The effect of intake valve alignment on swirl generation in a DI diesel engine. *Exp. Ther. Fluid Sci.*, 1999, **20**(2), 94–103.
7 **Bicen, A. F., Vafidis, C.** and **Whitelaw, J. H.** Steady and unsteady air flow through an intake valve of a reciprocating engine. *J. Fluids Engng*, 1985, **107**, 413–419.
8 **Floch, A., Dupont, A.** and **Baby, X.** In-cylinder flow investigation in a gasoline direct injection four valve engine: bowl shape piston effects on swirl and tumble motions. In FISITA Congress, Paris, France, 1998, paper F98T049.
9 **Aiyoshizawa, E., Muranaka, S., Kawashima, J.** and **Kimura, S.** Development of new 4-valve/cylinder small DI diesel engine. *JSAE Rev.*, 1999, **20**, 183–190.
10 **Lee, J., Kang, K., Choi, S., Jeon, C.** and **Chang, Y.** Flow characteristics and influence of swirl flow interactions on spray for direct injection diesel engine. In FISTA World Automotive Congress, Seoul, Korea, 2000, paper F2000A097.
11 **Bensler, H., Freek, C., Bensteen, B., Ritter, A.** and **Hentschel, A.** An experimental and numerical study

EN00004203 09-12-04 09:03:28 Rev 14.05
The Charlesworth Group, Huddersfield 01484 517077

of the steady-state flow of a SI-engine intake port. SAE technical paper 982470, 1998.

12 **Kim, Y.** and **Lee, K.** Three dimensional computation intake port and in-cylinder flow for different port shapes and various valve lifts in an SI engine. In Proceedings of the KSAE Conference, 1994, pp. 476–472.

13 **Xu, H.** Some critical technical issues on the steady flow testing of cylinder heads. SAE technical paper 2001-01-1308, 2001.

14 **Fitzgeorge, D.** and **Allison, J. L.** Air swirl in a road vehicle diesel engine. *Proc. Instn Mech. Engrs*, 1963–3, AD 4, 151–168.

15 **Oishi, Y., Otake, M.** and **Watanabe, Y.** Prediction of intake swirl applying CFD technique. In International Symposium on *Diagnostics and Modeling of Combustion in Internal Combustion Engines* (*COMODIA 94*), 1994.

16 **Corberán, J. M.** and **Pérez, R.** An alternative technique for swirl measurement. SAE technical paper 980486, 1998.

17 **Stone, C. R.** and **Ladommatos, N.** The measurement and analysis of swirl in steady flow. SAE technical paper 921642, 1992.

18 **Ricard.** Steady state flow bench port performance measurement and analysis techniques. Report DP93/0704, 1993.

19 **Hamamoto, Y., Tomita, E., Tanaka, Y.** and **Katayama, T.** The effect of swirl on spark-ignition engine combustion. In International Symposium on *Diagnostics and Modeling of Combustion in Internal Combustion Engines* (*COMODIA 94*), 1994.

APPENDIX

Notation

A_c	total curtain area
A_1	area in pressure measurement section
B	bore
C_e	discharge coefficient based on the curtain area
$C_{e,rel}$	relative flow ratio
C_{swirl}	Heywood swirl coefficient
DL	different lifts
G	mass flowrate through the ports
h_1	base lift
h_2	lift of valve 2
$\Delta h/h_1 = \Delta S/S_1$	throttling factor
k	isentropic coefficient
p_0	ambient pressure
p_1	downstream static pressure
S_r	swirl ratio
SCV	swirl control valve
V	engine's displacement
ρ_0	ambient density
ρ_1	air density in the pressure measurement section
ω	paddle-wheel rotational speed
ω_{mot}	crankshaft rotational speed

EN00004203 09-12-04 09:03:28 Rev 14.05
The Charlesworth Group, Huddersfield 01484 517077